Draft version August 21, 2026
Typeset using LaTeX twocolumn style in AASTeX7.0.2

Characterization of Brown Dwarf HD 176535B with KPIC

Vincent H. Hernandez,[1,2,3] Julianne Cronin,[2,3] and Jason J. Wang[2,3]

[1]Department of Physics and Astronomy, Williams College, Williamstown, MA 01267, USA
[2]Center for Interdisciplinary Exploration and Research in Astrophysics (CIERA), 1800 Sherman Ave., Evanston, IL 60201, USA
[3]Department of Physics and Astronomy, Northwestern University, 2145 Sheridan Rd, Evanston, IL 60208, USA

ABSTRACT

We present results from a characterization of the brown dwarf HD 176535B. Previous direct imaging studies on this brown dwarf have used photometric and low-resolution spectroscopy. However, we utilize Keck Planet Imager and Characterizer(KPIC) high-resolution spectroscopy to get detailed spectra from this brown dwarf. We used forward modeling techniques with the BT-Settl grid model to ascertain the parameters of this object. HD 176535B is a brown dwarf with a $T_{\rm eff}$ of 1496K, $\log(g)$ of 4.5, radial velocity of -29.59 km/s, and $v\sin(i)$ of -47.28km/s. With these parameters, we believe that HD 176535B is a late-L dwarf.

Keywords: Brown Dwarfs (185) — High Resolution Spectroscopy (2096) — Direct Imaging (387)

1. INTRODUCTION

Direct imaging technology has arguably been one of the most important advancements in exoplanet research. This technology can one day enable researchers to study Earth-sized exoplanets around Sun-like stars, and uncover the origins and extent of life as we know it.

Historically, substellar objects were observed indirectly, by observing the effects they have on their host star. With direct imaging, we are now able to directly detect the emission from these companions (T. Currie et al. 2023). Specifically, we are interested in studying exoplanets and brown dwarfs. The border between exoplanets and brown dwarfs is still debated. The major difference is in their formation. Brown Dwarfs form like stars, by collapsing gas, but lack the mass to ever undergo hydrogen fusion. Instead, they release energy by deuterium fusion, slowly cooling over their lifetime. Exoplanets form by accreting planetesimals, dust, and gas within their protoplanetary disks. This mechanism tends to divide them by mass at 13 $M_{\rm jup}$. (Y. Zhang et al. 2024a) For this paper, we will refer to these substellar objects collectively as companions. The companions themselves are usually compared to the planet Jupiter, as the companions we observe tend to be of similar scale or larger.

One of the major goals of spectroscopic analysis of substellar companions is to use atmospheric composition to infer the formation history of the object. For example, accurate C/O Values can constrain the contribution of planetesimal and pebble accretion. The ratio of different carbon molecules can also inform temperature estimates, as the prevailing form of carbon is temperature-dependent(P. Mollière et al. 2022). Overall, increasing the number of detailed characterizations from a sample of 32 companions(C.-C. Hsu et al. 2026), to a larger population can inform larger planet models, and help historical and statistical analyses to be more accurate(T. Currie et al. 2023).

To work towards this high-level analysis, we use the Keck Planetary Imager and Characterizer(KPIC), which was a modern direct imager and spectrometer connected to Keck II AO system, running from 2019-2025. As explained by J. J. Wang et al. (2021), this instrument utilizes a high-resolution spectrometer (R 35,000), allowing us to study individual absorption lines in a companion's emission spectrum. This data reveals Doppler shifts in the spectra to determine its radial velocity(RV). We can also gather information about specific molecular abundances, spin, and its orbit. KPIC studies in the K-band wavelength range, which is in the near infrared. Typically, the wavelengths 2.29-2.44μm are studied as it has many absorption lines from CO, H_2O, and CH_4, telling us a lot about the formation history, temperature, and atmospheric properties of the companion. KPIC uses single-mode fibers to counteract the glare from the host star, instead of a coronograph. The fiber injection unit(FIU) steers the light from the companion to disperse the light across the spectrograph. See Figure 1 for a visual of the fibers. This gives a narrow spectrum of

Corresponding author: Vincent H. Hernandez

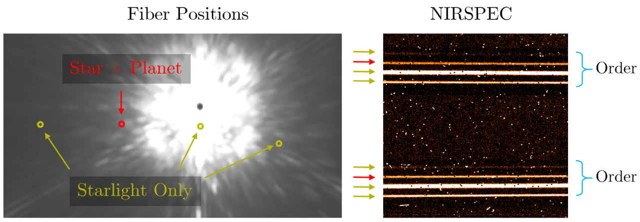

Figure 1. Figure 1 from Wang et al. 2021. Visual representation of KPIC observations. On the left are the locations of the hour fibers, relative to the host star, HD 8799. The red circle represents the fiber that is observing the companion, HD 8799c, and the yellow circles represent the unused fibers. Note that this image is photometric, and not used for spectroscopy. However, on the right is a part of a spectroscopic image. Here, two echelle orders are shown, with four spectra, corresponding to each of the four fibers shown.

just the light in that area, allowing for precise spectra from the companion and adequate noise reduction(J. J. Wang et al. 2021).

KPIC has been used to study many other exoplanet and brown dwarf companions, such as HD 8799bcde(J. J. Wang et al. 2021), HD 33632B(C.-C. Hsu et al. 2024), HD 7672AB(J. Wang et al. 2022), HD 4747B(J. W. Xuan et al. 2022), and HIP 99770B(Y. Zhang et al. 2024a). These studies use a combination of forward modeling with grid models and free retrieval with `petitRADTRANS`(P. Mollière et al. 2019) to characterize the companion and its atmosphere. We chose to study the brown dwarf HD 176535B(also known as HIP 93398 B) to build on previous low-resolution (B. L. Lewis et al. 2024) and photometric studies(Y. Li et al. 2023). HD 176535B also has a precisely determined dynamical mass, constraining one key parameter of the companion, allowing for more accurate modeling. There has been debate on the cloudiness and temperature of this companion, with B. L. Lewis et al. (2024) using low-resolution spectroscopy and a grid model to determine it has a higher temperature and cloudier atmosphere than Y. Li et al. (2023) had determined.

In this paper, we seek to use modern forward-modeling analysis to resolve conflicts between previous models and observations. In Section 2, we discuss the properties of the HD 176535 system and the research already done on this Brown Dwarf. In Section 3, we explain the observations and data processing. In Section 4, we explain the process of analyzing the data using forward models. Lastly, in Section 5 we discuss our results and what they say about our brown dwarf.

2. SYSTEM PROPERTIES

HD 176535B is a recently discovered brown dwarf with both spectroscopic and astrometric data. The host star, HD 176535, is a K-type star, with a mass of $0.72M_{\odot}$. The star has an effective temperature of 4727K, at a distance of 36.99pc (Y. Li et al. 2023). Further properties about the system can be found in Table 1, originally curated by Y. Li et al. (2023).

HD 176535B was initially analyzed by Y. Li et al. (2023), using Hipparcos–Gaia astrometry, High Accuracy Radial velocity Planet Searcher(HARPS) radial velocities, and KeckAO/NIRC2 L' Band direct imag-

Table 1. Properties of the HD 176535 AB system.

Property	Value	Refs.
Host star		
ϖ (mas)	27.033 ± 0.018	1
Distance (pc)	36.99 ± 0.03	1
SpT	K3.5V	2, 3
Mass ($M_{\odot}$)	0.72 ± 0.02	4, 5
Age (Gyr)	5.04 ± 1.45	10
$T_{\rm eff}$ (K)	4727 ± 104	6
[Fe/H] (dex)	-0.15 ± 0.07	7
Gaia RUWE	1.019	1
Luminosity ($L_{\odot}$)	0.208 ± 0.007	10
Gaia G (mag)	9.374 ± 0.003	1
B_T (mag)	11.195 ± 0.066	8
V_T (mag)	9.923 ± 0.035	8
J (mag)	7.804 ± 0.027	9
H (mag)	7.313 ± 0.033	9
K_s (mag)	7.175 ± 0.020	9
Companion		
Mass ($M_{\rm Jup}$)	$65.9^{+2.0}_{-1.7}$	10
Age (Gyr)	$3.59^{+0.87}_{-1.15}$	11
Radius(R_{Jup})	0.9 ± 0.03	11
L' apparent (mag)	16.31 ± 0.07	10
L' absolute (mag)	13.47 ± 0.07	10
Semimajor axis (au)	$11.05^{+0.64}_{-0.56}$	10
Inclination (°)	$49.8^{+3.4}_{-3.7}$	10
Period (yr)	$40.6^{+3.9}_{-3.5}$	10
Eccentricity	$0.496^{+0.022}_{-0.020}$	10

Note—References abbreviated as (1) A. G. A. Brown et al. (2021); (2) R. O. Gray et al. (2006); (3) L. Bourges et al. (2014); (4) A. Reiners & M. Zechmeister (2020)); (5) E. D. Mena et al. (2019) (6) S. G. Sousa et al. (2011); (7) A. Gáspár et al. (2016); (8) E. Høg et al. (2000); (9) R. M. Cutri et al. (2003); (10)Y. Li et al. (2023); (11)C.-C. Hsu et al. (2026)

ing data to constrain properties and run orbital fits on HD 176535B. A dynamical mass of $65.9^{+2.0}_{-1.7} M_{Jup}$ was constrained from the HARPS and Gaia Data. Effective temperatures($T_{\rm eff}$) and surface gravity($\log(g)$) values were derived using TUSCON, ATMO2020, and SM08 hybrid models, returning values in the range of 950K-988K and 5.19-5.32 cm s^{-2}, respectively. Their result was surprising, as the low temperature and high mass did not correlate with known evolutionary models for brown dwarfs.

Subsequently, a low-resolution spectroscopic analysis was done by B. L. Lewis et al. (2024) with the Subaru SCExAO/CHARIS instrument. They used low-resolution (R¡100) data taken in the broadband(J/H/K), J, and H bands with Sonora Diamondback models to determine that the $T_{\rm eff}$of HD 176535B is 1200K. This resolved our companion's tension with evolutionary models, and they labeled it as a cloudy L dwarf, near the L/T transition.

We followed up on these works by collecting spectroscopic data with the Keck Planet Imager and Characterizer(KPIC). Our goal was to use this high-resolution spectroscopic data to refine the physical parameters of HD176535B such as $T_{\rm eff}$and $\log(g)$, characterize its atmosphere, and understand its chemical makeup and properties.

3. OBSERVATIONS AND DATA PROCESSING

When observing with KPIC, we image the companion, the host star, an M Giant star that we use for wavelength calibration, and a telluric star that is an A0V spectral type. Telluric stars are used as a reference to see the absorption lines from molecules in Earth's atmosphere. To do this, we compare its spectra against those of accurately modeled spectra of these stars, usually PHOENIX models(T.-O. Husser et al. 2013). Any differences between the spectra we model and our observations are from Earth's atmosphere. The M Giant stars have very sharp, deep, and predictable CO lines. We use the location of these distinct lines on the detector to correlate physical position and spacing with wavelength. Table 2 lists the specific stars we observed and the number of observations, which were all taken on 09/25/24.

When observing, we alternated between fibers 2 and 4 when imaging our host star and companion. This also allows us to use nod subtraction, instead of background subtraction. Background subtraction requires taking dark images, which are images with the same exposure settings as the science image, but with no light. This captures background flux, which for KPIC mostly comes as thermal background from the instrument (J. J. Wang et al. 2021). However, KPIC's unique instrumentation allows for using nod subtraction. This uses alternating pairs of images, where the companion moves between two fibers. By subtracting these images from each other, you subtract the shared background and are left with an image with two spectra, one positive and one negative. Not taking dark images increases observation efficiency and is the preferred method of background subtraction for KPIC, which we use here.

To extract the spectra from the raw data, we follow the same processes described in (J. J. Wang et al. 2021). This uses the Python data reduction pipeline created by the KPIC team, hereafter referred to as `kpicdrp`[4]. This process first removes background, using nod subtraction, and bad pixels from the spectroscopic data. Then it extracts the fluxes from each fiber, in each order, to create spectra for each image. Lastly, we use the M giant star to create a wavelength calibration, which we then apply to all the spectra to properly label positions with wavelengths.

After processing the raw data, we prepared to run a cross-correlation with a similar model spectrum to prove there is a companion in the data and identify any anomalous images. We began sorting images of both the host star and companion by the fiber the image was taken with. In our case, we used KPIC science fibers 2 and 4. In this step, we identified two images of the companion, one from fiber, taken back to back, that had poor data quality that would interfere with future analysis. When included, these images caused the cross-correlation to fail. Upon visual inspection, we saw their spectra resembled the background, and not the companion. We were confident that these images were not suitable for further analysis, so we removed them from our data pool. We then were able to calculate the mean fluxes for each fiber. With the mean spectra, we ignored data outside the relevant orders we are studying(echelle orders 31 (2.44–2.49 μm), 32 (2.36–2.41 μm), and 33 (2.29–2.34 μm)). We then calculated a response curve based on the telluric star HD 182761 and a corresponding PHOENIX model(T.-O. Husser et al. 2013) to account for the effects of Earth's atmosphere on the spectra. Finally, we ran a cross-correlation against a BT-Settl model, with $T_{\rm eff}$=1000K and $\log(g)$=5.5, which is close to the anticipated values from Y. Li et al. (2023). The cross-correlation function (CCF) compares the model to the data to search for alignment of the absorption features in both spectra across a range of radial velocities. If the spectra are correlated, there should be a clear peak

[4] https://github.com/kpicteam/kpic_pipeline/

Table 2. Observations

Object	Purpose	Number of Images taken	Total Integration Time
HD 176535B	Target	11(9)[a]	5988.5(5090.22)[a]
HD 176535	Host Star	9	778.80
HIP 95771	Wave Cal	12	17.7
HD 182761	Telluric	8	472.0

[a]We removed two images of the companion, as they were determined to be of poor quality and/or non-detections. See below for further explanation.

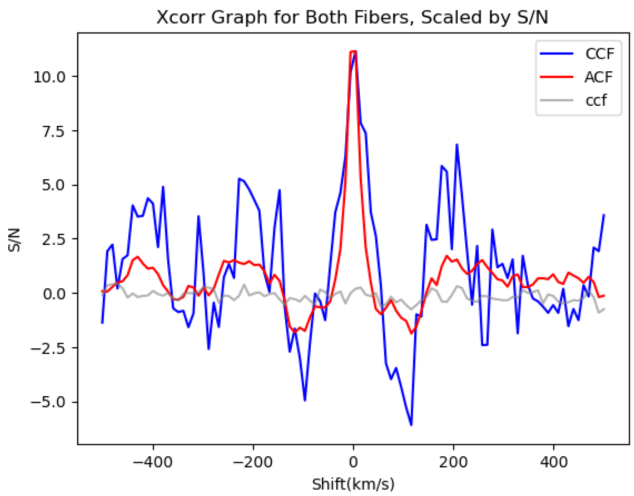

Figure 2. Cross-correlation result against a BT-Settl model with $T_{\rm eff}$=1000K and log(g)=5.5, against all data, scaled by SNR with a background fiber for noise reference.

near the host star's RV, or, in our case, at 0km/s shift for data that is already RV shifted. We also plotted an auto-correlation function, which runs a CCF with the data against itself, to ensure consistency. We also expect a peak at 0 km/s here. Lastly, we ran a CCF against a background fiber with no data, where we expect to see only noise. This ensures that our detections are actually detecting the companion and not a background object. It also allows us to scale our CCF and ACF by the noise to get an SNR value. The resulting plot, Figure 2, shows a clear spike in the cross CCF and ACF at 0km/s, with a peak SNR of 11.73, signifying a successful cross-correlation and detection of HD 176535B.

4. FORWARD MODELING

Even with an instrument as high-resolution and sensitive as KPIC, we still cannot isolate the planet's spectra from the glare of the star it is orbiting. To determine the properties of HD 176535B we instead use a technique called forward modeling. Here, we use a pre-computed grid of brown dwarfs with varying parameters. We add onto this spectra the mean light from the host star, and we redshift it and rotationally broaden the spectrum, based on the radial velocity(RV) and rotational velocity ($v\sin(i)$) we are fitting for. This process returns modeled spectra that closely represents the data we get from KPIC. We do this process over and over again, until we find the input parameters that best match our data.

For our forward modeling, we used the BT-Settl(F. Allard 2013) model grid to determine the effective temperature($T_{\rm eff}$), surface gravity (log(g)), RV and $v\sin(i)$of HD 176535B. BT-Settl is a pre-computed, self-consistent, cloudy 1D radiative-convective grid model. Beyond these parameters, we also fit for an LSFσ parameter, which is the error caused by the instrument, specifically the broadening on monochromatic lines from the optics. It also serves to match the model's spectral resolution to the data. Lastly, we fit for a logarithmic Error jitter parameter for each order, to inflate the error as we assume our errors found by $\sigma = \frac{1}{\sqrt{N}}$ are underestimates. Therefore, we define our errors according to Equation 1.

$$\text{Error} = \sqrt{\sigma^2 + (e^{\text{jitter}})^2} \tag{1}$$

We used Bayesian inference to constrain the model parameters that best reproduce our data. Our log-like function takes the model from an interpolated grid. It then rotationally broaden it with the `rotBroadInt` function from the `kpicdrp` package, and use `generate_forward_model_singleorder` from the same package to apply the RV shift and the influence of Earth's atmosphere to generate the forward model. The last step is to remove the blackbody continuum of the planet through `scipy`'s `median_filter`, with a width of 100 pixels. Finally, it runs a χ^2 goodness-of-fit test on each model against the data and returns the likelihood.

We used nested sampling with `dynesty` to evaluate our models and generate posterior distributions. Nested sampling begins by distributing points across the hypercube made from all the parameters in the prior. The number of live points used requires a balance between minimizing compute time and having enough points to accurately map the posterior. In our case, we used 512 points. The algorithm then runs our log-likelihood function for each point and removes the point with the lowest log-likelihood. Our log likelihood equation is given in Equation 2 (J.-B. Ruffio et al. 2019) where F is the flux marginalization constant and σ is the inflated errors across all orders. The nested sampling algorithm then randomly places a new point in the volume bounded by the remaining points, keeping it if it has a likelihood that is higher than the point that it is replacing. After each iteration, it estimates the remaining evidence and stops when it hits a threshold, in our case, $\Delta logZ < .521$, as suggested by dynesty[5].

$$ln(\mathcal{L}) = -\frac{1}{2}\sum\left(\frac{(\text{Data} - \text{Model})^2}{\sigma^2} + \ln(2\pi\sigma^2)\right) + F \tag{2}$$

5. RESULTS, ANALYSIS, AND DISCUSSION

After the completion of nested sampling, our analysis returned the posterior, as shown in Figure 3. Table 3. shows the corresponding best-fit values, as well as those found by Y. Li et al. (2023). Through our forward modeling process, we found that HD 176535B has a $T_{\text{eff}}$of $1496^{+6.75}_{-11.76}K$, a $\log(g)$of $4.50^{+0.04}_{-0.05}$, an RV of $-29.59^{+2.82}_{-2.45}$ km/s, and a $v\sin(i)$of $47.28^{+4.91}_{-4.41}$ km/s. We used these values to generate a our best-fit model spectra, in the same way as detailed in section 4. We compare this to the data in 3.

As a sanity check, we compared our modeled Radial Velocity to that of HD 176535A, the host star. This value was found to be -31. 743, from the Gaia survey(C. Soubiran et al. 2018). Using the period, semi-major axis, eccentricity, and inclination from Y. Li et al. (2023), we use Equation 3 to estimate the maximum RV offset the companion will have. We find this upper limit to be 7 km/s, which agrees with our findings. C.-C. Hsu et al. (2026) used a similar forward modeling process in their survey on companion spins, and found a value of 37.6, which is within 2σ of our findings. In the future, we want to explore the slight discrepancy between these spin values to understand if it is caused by a systematic error, a poor fit of the value, or a difference in preferred solutions from different model grids.

A Brown Dwarf of 1496 K is likely a late-L Brown Dwarf. In high-resolution spectra, this temperature comes from comparing depths of CO absorption lines

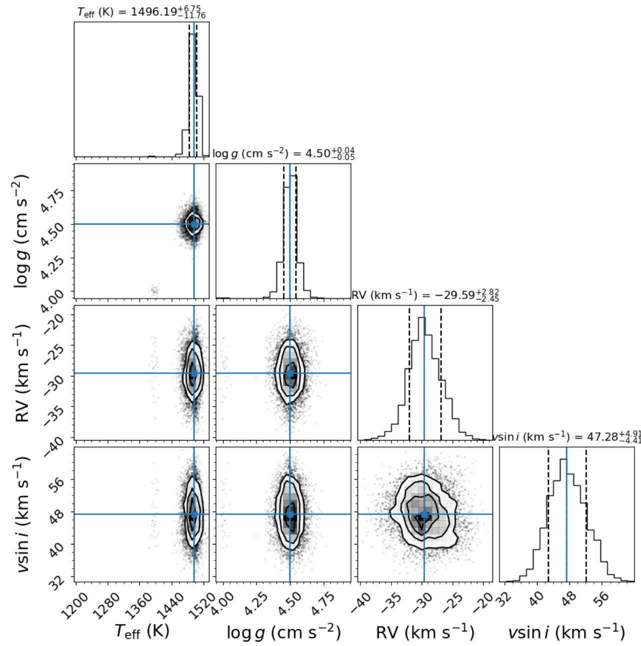

Figure 3. A corner plot showing the posterior distributions for T_{eff}(K), $\log(g)$(log(m/s)), RV(km/s), and $v\sin(i)$ in the BT-Settl model.

to CH_4. However, BT-Settl models tend to overestimate temperatures, as they assume equilibrium chemistry (A. Sanghi et al. (2023), Section 8.3.1.) We believe this is because in a Brown Dwarf's photosphere CO and H_2O can react to form CH_4. However, in the deeper layers of the atmosphere, this conversion cannot occur, as the temperature is too high. Typically, there is vertical mixing, where the warmer gas containing CO is carried to the upper atmosphere, reducing the CH_4 in these layers. (CITE) Without accounting for this vertical mixing, BT-Settl sees the closer ratio of CO to CH_4 at the outer layers as a warmer Brown Dwarf. We would confirm this by performing a more detailed characterization and calculating a higher ratio of CO to CH_4. In the future, it would also be advantageous to run a second high-resolution model grid with a vertical mixing parameter to accurately predict this phenomenon. We look forward to the release of High-Resolution Exo-REM Models for this purpose(A. Radcliffe et al. 2026).

$$K_{\text{rel}} = \frac{2\pi a \sin i}{P\sqrt{1-e^2}} \tag{3}$$

We are preparing to run a free-retrieval with `petitRADTRANS` on our data for future analysis. `petitRADTRANS` is similar to our previous grid-based approach, but does not use a pre-computed grid. Instead, we create the atmosphere from scratch, layer by layer. Within each layer, we can control many factors, such as chemical abundances, the temperature/pressure pro-

[5] The equation they use is $.001 * (nlive - 1) + 0.01$. For our 512 live points, this returns .521.

Table 3. Best Fit Parameters from BT-Settl

Parameter	Prior	Our Best Fit	From Y. Li et al. (2023)	From B. L. Lewis et al. (2024)
$T_{\rm eff}$(K)	700-1700	$1496^{+6.75}_{-11.76}$	980 ± 35	1200^{+140}_{-119}
$\log(g)$(m/s)	3.5-5.5	$4.50^{+0.04}_{-0.05}$	$5.30 \pm .06$	5.0
RV(km/s)	-70-0	$-29.59^{+2.82}_{-2.45}$	N/A	N/A
$v\sin(i)$(km/s)	0-100	$47.28^{+4.91}_{-4.41}$	N/A	N/A
Spectral Type	N/A	Late-L	T6	L9

Note—Each of our priors was distributed uniformly.

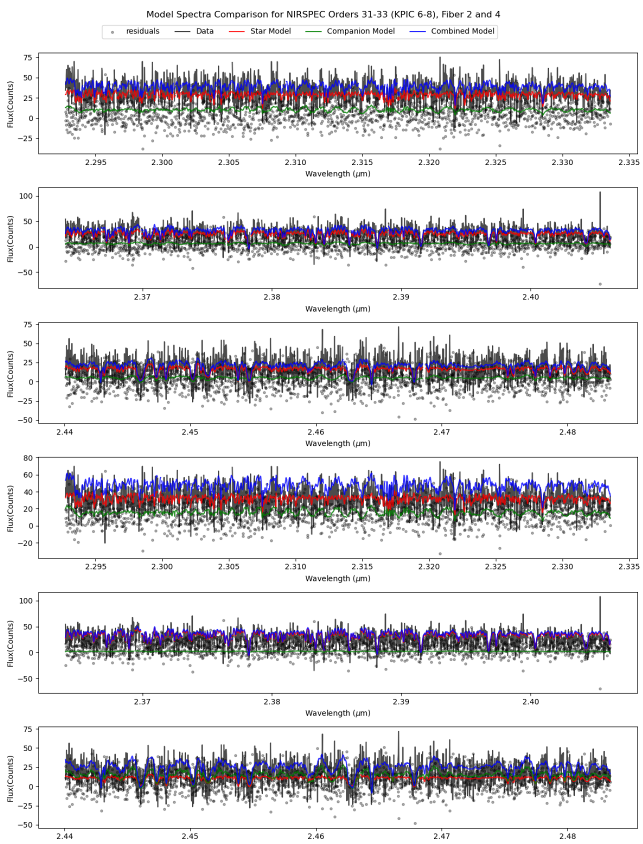

Figure 4. Plots comparing the spectra of the companion, star, and combined models to the observed spectra of HD 176535B. All Spectra have been median filtered. Top: Fiber 2, Orders 6,7,8. Bottom: Fiber 4, Order 6,7,8

file, and chemical mixing ratios. Then the light that makes it through the layer from the one below is calculated. Ultimately, we get a spectrum similar to grid based model. However, we also have many more parameters which provide deeper insight into the composition and atmospheric characteristics on the companion.

6. CONCLUSION

HD 176535B is a brown dwarf that was first found to be an early-mid T dwarf(Y. Li et al. 2023) with a $T_{\rm eff}$980K. A subsequent study found it to actually be a late L-dwarf, with a $T_{\rm eff}$1200K(B. L. Lewis et al. 2024). To build on these studies, we used KPIC to perform a high resolution spectrographic study on HD 176535B. We used a grid-based forward modeling approach with BT-Settl to find that HD 176535B has a $T_{\rm eff}$of 1496K, a $\log(g)$of 4.50, an RV of -29.59 km/s, and a $v\sin(i)$of 47.28 km/s. We agree that this is a late-L brown dwarf, and found our RV to be consistent with Gaia studies on its host star. We anticipate that our future analysis of HD 176535B with `petitRADTRANS` will yield more insight into its chemical composition and internal properties, adding it to the list of well parameterized, directly-imaged substellar objects.

ACKNOWLEDGMENTS

This material is based upon work supported by the U.S. National Science Foundation under Award No. AST-2446392. V.H would like to thank Julianne Cronin and Jason Wang for their time and effort as his REU advisors. He would also like to thank L. Cliff Johnson and Mark Gorski for directing the CIERA REU, of which this work is a result of. Funding for KPIC has been provided by the California Institute of Technology, the Jet Propulsion Laboratory, the Heising-Simons Foundation (grants #2015-129, #2017-318, #2019-1312, and #2023-4598), the Simons Foundation (through the Caltech Center for Comparative Planetary Evolution), and the NSF under grant AST1611623. Data presented herein were obtained at the W. M. Keck Observatory, which is operated as a scientific partnership among the California Institute of Technology, the University of California, and the National Aeronautics and Space Administration. The Observatory was made possible by the generous financial support of the W. M. Keck Foundation. The authors recognize and acknowledge the significant cultural role and reverence that the summit of Maunakea has with the indigenous Hawaiian community, and that the W. M. Keck Observatory stands on Crown and Government Lands that the State of Hawai'i is obligated to protect and preserve for future generations of indigenous Hawaiians. This research was supported in part through the computational resources and staff contributions provided for the Quest high performance computing facility at Northwestern University which is jointly supported by the Office of the Provost, the Office for Research, and Northwestern University Information Technology.This work used computing resources provided by Northwestern University and the Center for Interdisciplinary Exploration and Research in Astrophysics (CIERA).

Facilities: Keck II: (NIRSPEC)

Software: `Astropy` (The Astropy Collaboration et al. 2013, 2018, 2022), `corner` (D. Foreman-Mackey 2016), `DYNESTY` (J. S. Speagle 2020; S. Koposov et al. 2026; J. Skilling 2004, 2006; F. Feroz et al. 2009; R. M. Neal 2003; W. J. Handley et al. 2015a,b), `h5py` (A. Collette 2013), `KPICDRP` (J. J. Wang et al. 2021), `Matplotlib` (T. M. D. Team 2026), `Numpy` (C. R. Harris et al. 2020), `petitRADTRANS` (P. Mollière et al. 2019), and `Scipy` (P. Virtanen et al. 2020).

REFERENCES

Allard, F. 2013, Proceedings of the International Astronomical Union, 8, 271, doi: 10.1017/S1743921313008545

Bourges, L., Lafrasse, S., Mella, G., et al. 2014, Astronomical Data Analysis Software and Systems XXIII, 485, 223

Brown, A. G. A., Vallenari, A., Prusti, T., et al. 2021, Astronomy & Astrophysics, 649, A1, doi: 10.1051/0004-6361/202039657

Collette, A. 2013, Python and HDF5 (O'Reilly)

Currie, T., Biller, B., Lagrange, A.-M., et al. 2023, Direct Imaging and Spectroscopy of Extrasolar Planets, arXiv, doi: 10.48550/arXiv.2205.05696

Cutri, R. M., Skrutskie, M. F., van Dyk, S., et al. 2003, VizieR Online Data Catalog, 2246, II/246. https://ui.adsabs.harvard.edu/abs/2003yCat.2246....0C

Feroz, F., Hobson, M. P., & Bridges, M. 2009, Monthly Notices of the Royal Astronomical Society, 398, 1601, doi: 10.1111/j.1365-2966.2009.14548.x

Foreman-Mackey, D. 2016, The Journal of Open Source Software, 1, 24, doi: 10.21105/joss.00024

Gray, R. O., Corbally, C. J., Garrison, R. F., et al. 2006, The Astronomical Journal, 132, 161, doi: 10.1086/504637

Gáspár, A., Rieke, G. H., & Ballering, N. 2016, The Astrophysical Journal, 826, 171, doi: 10.3847/0004-637X/826/2/171

Handley, W. J., Hobson, M. P., & Lasenby, A. N. 2015a, Monthly Notices of the Royal Astronomical Society, 450, L61, doi: 10.1093/mnrasl/slv047

Handley, W. J., Hobson, M. P., & Lasenby, A. N. 2015b, Monthly Notices of the Royal Astronomical Society, 453, 4384, doi: 10.1093/mnras/stv1911

Harris, C. R., Millman, K. J., Van Der Walt, S. J., et al. 2020, Nature, 585, 357, doi: 10.1038/s41586-020-2649-2

Hsu, C.-C., Wang, J. J., Xuan, J. W., et al. 2024, The Astrophysical Journal, 971, 9, doi: 10.3847/1538-4357/ad58d3

Hsu, C.-C., Wang, J. J., Xuan, J. W., et al. 2026, The Astronomical Journal, 171, 224, doi: 10.3847/1538-3881/ae434b

Husser, T.-O., Berg, S. W.-v., Dreizler, S., et al. 2013, Astronomy & Astrophysics, 553, A6, doi: 10.1051/0004-6361/201219058

Høg, E., Fabricius, C., Makarov, V. V., et al. 2000, Astronomy and Astrophysics, 355, L27. https://ui.adsabs.harvard.edu/abs/2000A&A...355L..27H

Koposov, S., Speagle, J., Barbary, K., et al. 2026, joshspeagle/dynesty: v3.1.0, Zenodo, doi: 10.5281/ZENODO.3348367

Lewis, B. L., Li, Y., Gibbs, A., et al. 2024, The Astrophysical Journal, 977, 247, doi: 10.3847/1538-4357/ad90bc

Li, Y., Brandt, T. D., Brandt, G. M., et al. 2023, Monthly Notices of the Royal Astronomical Society, 522, 5622, doi: 10.1093/mnras/stad1315

Mena, E. D., Moya, A., Adibekyan, V., et al. 2019, Astronomy & Astrophysics, 624, A78, doi: 10.1051/0004-6361/201834783

Mollière, P., Wardenier, J. P., Boekel, R. v., et al. 2019, Astronomy & Astrophysics, 627, A67, doi: 10.1051/0004-6361/201935470

Mollière, P., Molyarova, T., Bitsch, B., et al. 2022, The Astrophysical Journal, 934, 74, doi: 10.3847/1538-4357/ac6a56

Neal, R. M. 2003, The Annals of Statistics, 31, doi: 10.1214/aos/1056562461

Radcliffe, A., Charnay, B., Lagrange, A.-M., et al. 2026, Astronomy & Astrophysics, 711, A257, doi: 10.1051/0004-6361/202659006

Reiners, A., & Zechmeister, M. 2020, The Astrophysical Journal Supplement Series, 247, 11, doi: 10.3847/1538-4365/ab609f

Ruffio, J.-B., Macintosh, B., Konopacky, Q. M., et al. 2019, The Astronomical Journal, 158, 200, doi: 10.3847/1538-3881/ab4594

Sanghi, A., Liu, M. C., Best, W. M. J., et al. 2023, The Astrophysical Journal, 959, 63, doi: 10.3847/1538-4357/acff66

Skilling, J. 2004, AIP Conference Proceedings, 735, 395, doi: 10.1063/1.1835238

Skilling, J. 2006, Bayesian Analysis, 1, doi: 10.1214/06-BA127

Soubiran, C., Jasniewicz, G., Chemin, L., et al. 2018, Astronomy & Astrophysics, 616, A7, doi: 10.1051/0004-6361/201832795

Sousa, S. G., Santos, N. C., Israelian, G., Mayor, M., & Udry, S. 2011, Astronomy & Astrophysics, 533, A141, doi: 10.1051/0004-6361/201117699

Speagle, J. S. 2020, Monthly Notices of the Royal Astronomical Society, 493, 3132, doi: 10.1093/mnras/staa278

Team, T. M. D. 2026, Matplotlib: Visualization with Python, Zenodo, doi: 10.5281/ZENODO.592536

The Astropy Collaboration, Robitaille, T. P., Tollerud, E. J., et al. 2013, Astronomy & Astrophysics, 558, A33, doi: 10.1051/0004-6361/201322068

The Astropy Collaboration, Price-Whelan, A. M., Sipőcz, B. M., et al. 2018, The Astronomical Journal, 156, 123, doi: 10.3847/1538-3881/aabc4f

The Astropy Collaboration, Price-Whelan, A. M., Lim, P. L., et al. 2022, The Astrophysical Journal, 935, 167, doi: 10.3847/1538-4357/ac7c74

Virtanen, P., Gommers, R., Oliphant, T. E., et al. 2020, Nature Methods, 17, 261, doi: 10.1038/s41592-019-0686-2

Wang, J., Kolecki, J. R., Ruffio, J.-B., et al. 2022, The Astronomical Journal, 163, 189, doi: 10.3847/1538-3881/ac56e2

Wang, J. J., Ruffio, J.-B., Morris, E., et al. 2021, The Astronomical Journal, 162, 148, doi: 10.3847/1538-3881/ac1349

Xuan, J. W., Wang, J., Ruffio, J.-B., et al. 2022, The Astrophysical Journal, 937, 54, doi: 10.3847/1538-4357/ac8673

Zhang, Y., Xuan, J. W., Mawet, D., et al. 2024a, The Astronomical Journal, 168, 131, doi: 10.3847/1538-3881/ad6609